

2005

## Temporal change detection using ASTER and USGS digital elevation models

Pascal G. Akl  
*San Jose State University*

Follow this and additional works at: [https://scholarworks.sjsu.edu/etd\\_theses](https://scholarworks.sjsu.edu/etd_theses)

---

### Recommended Citation

Akl, Pascal G., "Temporal change detection using ASTER and USGS digital elevation models" (2005).  
*Master's Theses*. 2810.

DOI: <https://doi.org/10.31979/etd.kg2x-344q>  
[https://scholarworks.sjsu.edu/etd\\_theses/2810](https://scholarworks.sjsu.edu/etd_theses/2810)

This Thesis is brought to you for free and open access by the Master's Theses and Graduate Research at SJSU ScholarWorks. It has been accepted for inclusion in Master's Theses by an authorized administrator of SJSU ScholarWorks. For more information, please contact [scholarworks@sjsu.edu](mailto:scholarworks@sjsu.edu).

TEMPORAL CHANGE DETECTION USING ASTER AND USGS DIGITAL  
ELEVATION MODELS

A Thesis

Presented to

The Faculty of the Department of Geography

San Jose State University

In Partial Fulfillment

Of the Requirements for the Degree

Master of Arts

by

Pascal G. Akl

May 2005

UMI Number: 1431292

Copyright 2005 by  
Akl, Pascal G.

All rights reserved.

## INFORMATION TO USERS

The quality of this reproduction is dependent upon the quality of the copy submitted. Broken or indistinct print, colored or poor quality illustrations and photographs, print bleed-through, substandard margins, and improper alignment can adversely affect reproduction.

In the unlikely event that the author did not send a complete manuscript and there are missing pages, these will be noted. Also, if unauthorized copyright material had to be removed, a note will indicate the deletion.

**UMI<sup>®</sup>**

---

UMI Microform 1431292

Copyright 2005 by ProQuest Information and Learning Company.

All rights reserved. This microform edition is protected against  
unauthorized copying under Title 17, United States Code.

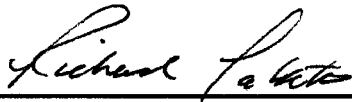
ProQuest Information and Learning Company  
300 North Zeeb Road  
P.O. Box 1346  
Ann Arbor, MI 48106-1346

© 2005

Pascal G. Akl

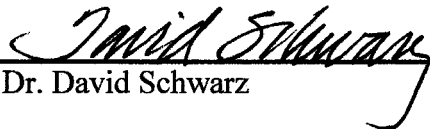
All rights reserved

APPROVED FOR THE DEPARTMENT OF GEOGRAPHY

A handwritten signature in cursive script, appearing to read "Richard Taketa".

---

Dr. Richard Taketa

A handwritten signature in cursive script, appearing to read "David Schwarz".

---

Dr. David Schwarz

A handwritten signature in cursive script, appearing to read "Gary Pereira".

---

Dr. Gary Pereira

APPROVED FOR THE UNIVERSITY

A handwritten signature in cursive script, appearing to read "Rhea I. Williamson".

## ABSTRACT

### TEMPORAL CHANGE DETECTION USING ASTER AND USGS DIGITAL ELEVATION MODELS

by Pascal G. Akl

The Advanced Spaceborne Thermal Emission and Reflection Radiometer (ASTER) has stereo capabilities that allow generating high resolution digital elevation model (DEM) similar in specification to that of the USGS 7.5 minute DEM and the National Elevation Dataset. ASTER data is more current (February 2000) than the USGS data (1925-1999), an important advantage for revealing surface temporal elevation changes. For this study, one ASTER DEM Granule (60Km x 60 Km) was selected and acquired, and USGS elevation data for the same area were acquired. The DEMs were standardized to the same projection and resolution and compared on a pixel-by-pixel basis to measure elevation differences. The accuracy and RMSE of the datasets were measured to outline the elevation differences to be considered significant for change detection. Temporal elevation changes were detected in the study area, and a history and field inspection revealed the reasons for the surface change.

## ACKNOWLEDGMENTS

My sincere thanks to my professors and thesis committee: my advisor Dr. Richard Taketa, Dr. David Schwarz, and Dr. Gary Pereira for all the valuable lessons they taught me during the course of my Master degree program.

I thank my parents, my brother, and my sister for their encouragement and support in each major step I took in my life. Thank you for being always there for me.

My deep sense of gratitude goes to my wife, Mihaela. Thank you for your patience and loving support. I dedicate this work to you and to our children.

## TABLE OF CONTENTS

	Page
ABSTRACT.....	iv
ACKNOWLEDGMENTS .....	v
LIST OF TABLES.....	viii
LIST OF FIGURES .....	ix
1. INTRODUCTION .....	1
2. STUDY AREA .....	3
3. DATASETS OVERVIEW AND ACQUISITION .....	4
3.1. ASTER Instrument and Data .....	4
3.1.1. ASTER DEM Acquisition .....	6
3.1.2. Ground Control Points .....	7
3.2. USGS 7.5 minute DEM .....	12
3.2.1. 7.5 minute DEM Acquisition.....	13
3.2.2. SDTS Import and DEM Mosaicking .....	13
3.3. National Elevation Dataset (NED).....	14
4. DATA PREPARATION FOR INSPECTION AND ANALYSIS .....	16
5. DATA INSPECTION AND QUALITY ASSESSMENT - EXPLORING THE DEMS .....	17
5.1. Comparison of DEM Data with High Accuracy Control Points.....	17
5.2. Flaws in ASTER Absolute DEM.....	18
6. ELEVATION CHANGE DETECTION APPROACH .....	21



6.1. Statistical Assessment of the Variance between ASTER and USGS DEMs	22
6.2. Temporal Elevation Change Detection -- Visual Inspection .....	23
7. RESULTS AND DISCUSSION .....	28
7.1. False Difference Deriving from Products Accuracy .....	28
7.2. True Difference from Land Cover .....	29
7.3. True Difference from Temporal Changes .....	30
8. CONCLUSION .....	37
REFERENCES .....	39
APPENDIX A TRIMBLE GEOEXPLORER III CONFIGURATION FOR FIELD	
SURVEY .....	42
APPENDIX B GROUND CONTROL POINTS USED FOR ASTER ABSOLUTE	
DEM GENERATION .....	43

## LIST OF TABLES

Table 1. Acquired DEMs original projection and resolution.....	16
Table 2. Statistical results: root mean square (RMS) and maximum elevation errors of the DEMs computed with 76 control points .....	18
Table 3. Statistical results (in meters) of elevation differences between the ASTER- extracted DEM and the USGS DEMs.....	23
Table 4. Location of temporal elevation changes detected and identified.....	32

## LIST OF FIGURES

Figure 1. ASTER granule coverage / study site.....	3
Figure 2. ASTER spectral bands.....	4
Figure 3. ASTER VNIR subsystem .....	5
Figure 4. Distribution of ground control points used for ASTER DEM generation.....	9
Figure 5. Locating distinct features on ASTER 3N and 3B bands using Freeview, and planning the GPS field survey .....	10
Figure 6. Transect profile over Calaveras reservoir and surrounding area.....	20
Figure 7. Transect profile over San Francisco Bay, from East Palo Alto to Newark city	20
Figure 8. Histogram analysis showing a normal distribution in elevation differences when comparing every pixel of ASTER DEM with that of a USGS 7.5' raster .....	22
Figure 9. Min-max histogram stretch of the variance raster between ASTER and the 7.5' elevation mosaic (VR ASTER-7.5').....	26
Figure 10. Classification of the natural logarithm of VR ASTER-NED .....	27
Figure 11. Land cover elevation difference detection .....	29
Figure 12. Hanson quarry detection and elevation change assessment .....	33
Figure 13. Landfills detection and relief change evaluation in Byron Hot Springs quad.	34
Figure 14. Coyote Hills Quarry detection on the coast, in Newark quad .....	35
Figure 15. Newby Island Sanitary Landfill, Milpitas quad .....	36

## INTRODUCTION

Digital Elevation Model (DEM) data provide the basis for modeling and analysis of spatio-topographic information, from Earth Sciences and land surface research to practical engineering applications, planning, and resource management. In many applications, DEM data need to be accurate, high resolution, and up-to-date (Honda, 2004). Much of the US Geological Survey (USGS) DEM data are outdated. Using outdated DEMs where surfaces are disturbed by human activities or natural disasters could greatly alter results in watershed and flood analysis, or the level of accuracy of orthorectified imagery when an ideal reference image is desired.

The USGS distributes two types of high resolution DEM data: The original DEM 7.5 minute quad data, and the National Elevation Dataset (NED). Most of these data were generated based on old sources (as old as 1948 for this study) such as topographic maps or aerial photography. The original DEM 7.5 minute data are provided in tiles having the same coverage as a standard USGS 1:24,000-scale quadrangle map. As this study shows, gathering, mosaicking, and standardizing the DEM quads is a challenge when working with large areas. To facilitate scientific use of elevation data over large areas, the USGS has produced and is distributing the National Elevation Dataset (NED). NED has been developed by merging the highest-resolution, best quality elevation data available across the United States into a seamless raster format. It is updated bimonthly to incorporate the "best available" DEM data (USGS, 2002).

Since November of 2000, a new source of satellite data has been publicly available to the scientific community: ASTER (Advanced Spaceborne Thermal Emission

and Reflection Radiometer) that is orbiting the earth onboard the Terra satellite launched in December 1999 as part of NASA's Earth Observing System (EOS). The two stereo bands (3n and 3b) contained in ASTER Level 1A (L1A) data granule can be used to produce digital elevation models. The quality of this DEM data, as described in the ASTER product specification guide, seems to be equivalent in resolution and accuracy to the USGS 1:24,000-Scale (7.5-minute) DEM data.

Both ASTER and USGS DEMs typically have 30x30 meter grid spacing (resolution), which allows comparing the two over the same coverage area. Significant differences in elevations between the two datasets sources might reveal temporal changes since the ASTER DEM is more up-to-date than the USGS DEMs. The main objective of this research is to look into the potential of using ASTER DEM to detect temporal elevation changes in disturbed surfaces (e.g., landfills, quarries, major urban development projects) by comparing it to the USGS DEMs. The feasibility of this approach might help identify illegal dumping or excavation activities, or simply help identify outdated DEM sources. The study will also discuss differences between the two sources and the techniques needed to introduce them into a GIS and remote sensing environment.

## STUDY AREA

The study area shown in Figure 1 was chosen based on the availability of an adequate ASTER image (granule) covering a high concentration of disturbed surfaces within the Bay Area, mainly landfills. Landfill operations involve significant dynamic elevation changes over relatively short periods of time through cut and fills.

The granule acquired for this study covers mainly the East part of Alameda and the North half of Santa Clara counties. Only about 35% of the terrain in the study site is flat, mostly around the bay near sea level; the rest is characterized by a rugged topography with elevations reaching 1300 m, and a mean slope of 10° and up-to 51° slopes.

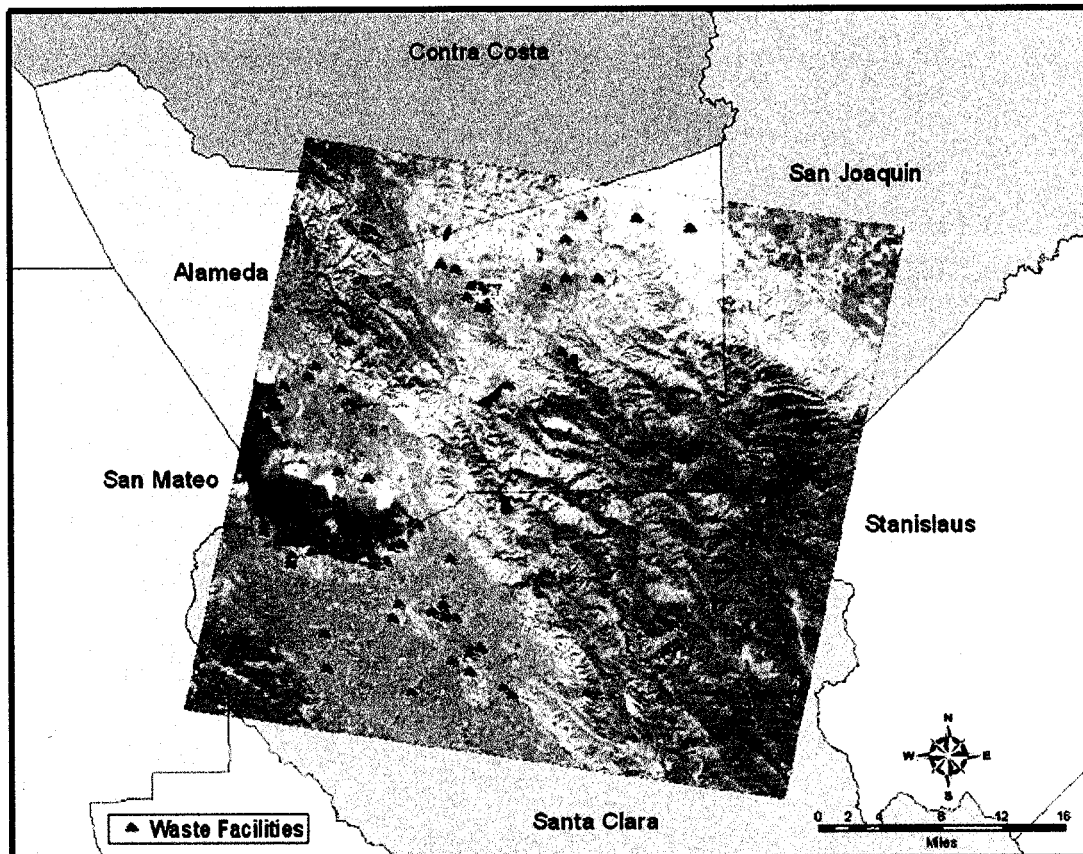


Figure 1. ASTER granule coverage / study site

## DATASETS OVERVIEW AND ACQUISITION

### ASTER Instrument and Data

The Advanced Spaceborne Thermal Emission and Reflection Radiometer (ASTER) is placed with four other high-tech instrument sensor systems (MODIS, MISR, CERES, and MOPITT) onboard NASA's Terra spacecraft that was launched in December 1999. It is the only high spatial-resolution instrument on the Terra platform. ASTER covers a wide spectral region (14 bands) using three different subsystems: visible and near infrared (VNIR) with 15-m resolution, the short-wave infrared (SWIR) with 30-m resolution, and thermal infrared (TIR) with 90-m resolution (Figure 2).

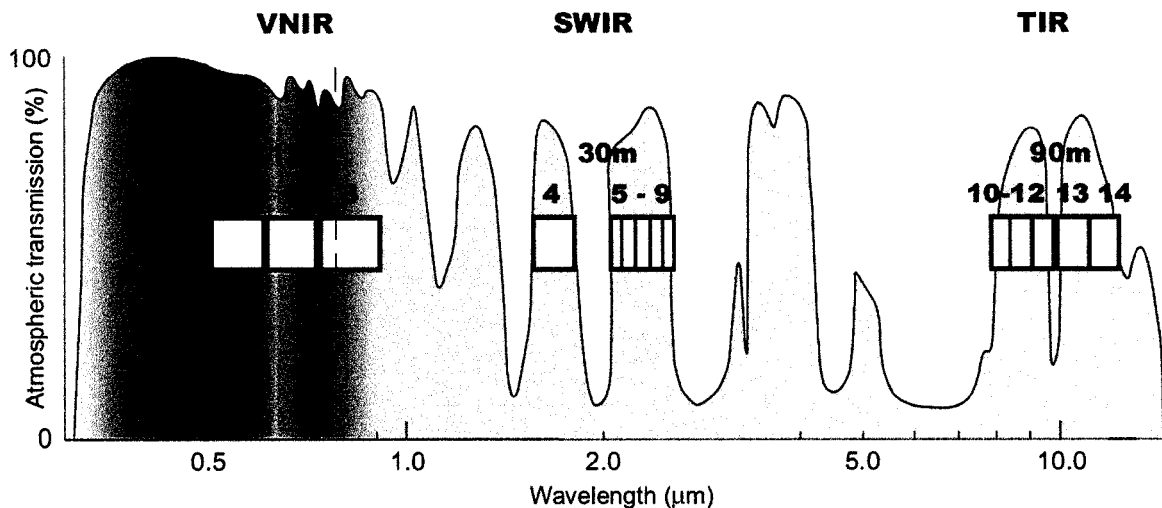


Figure 2. ASTER spectral bands

The red rectangular boxes indicate the sensor channels. The respective spatial resolution is indicated above the boxes. The colored curve in the background represents the atmospheric transmission in dependency on the wavelength. The vertical dashed line marks the approximate margin of visible light. (Modified from Graphic created by Dr. Andreas Kaeab, Department of Geography, University of Zurich).

The VNIR subsystem consists of two independent telescopes: the nadir telescope that contains three detector line arrays (Bands 1, 2, 3N), and the backward telescope that detects only one band (3B). The near infrared spectral bands, 3N and 3B, generate along-track stereo image pair with a base/height (B/H) ratio of 0.6, and an intersection angle of about 27.7 degrees (Figure 3).

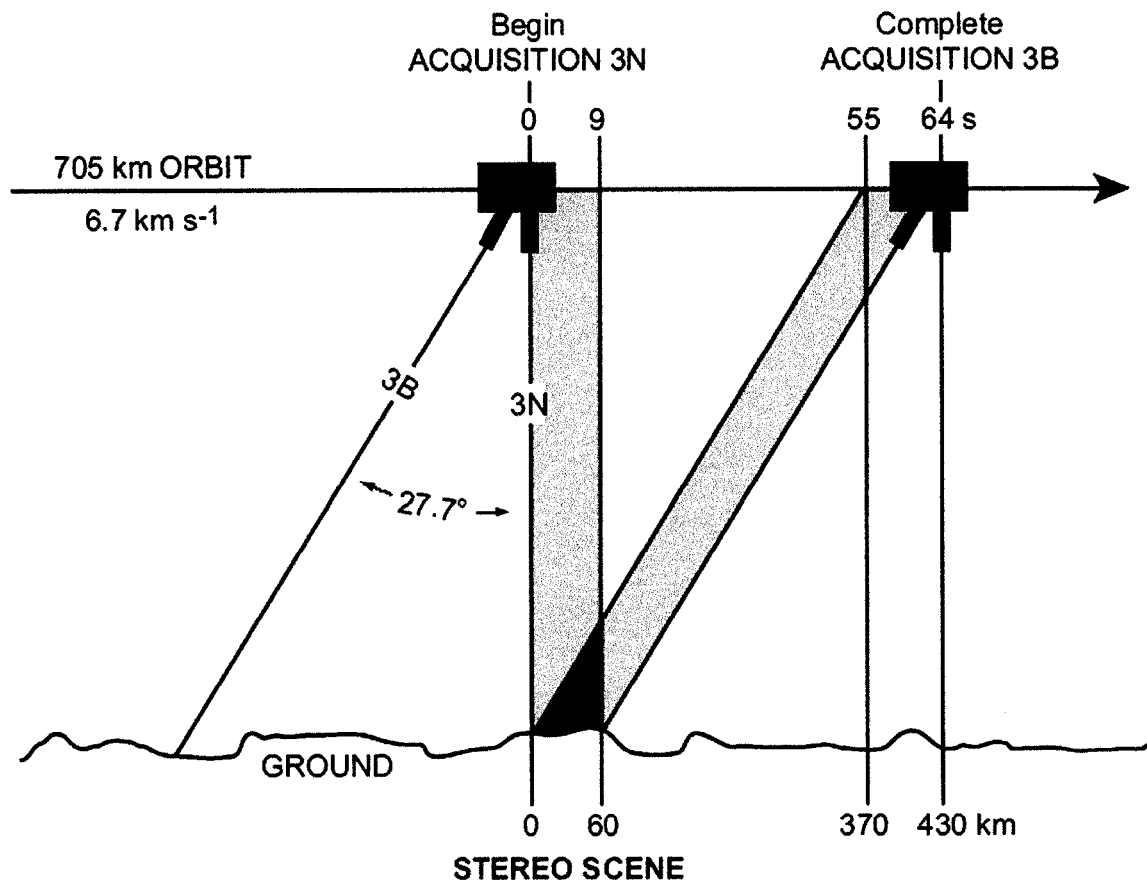


Figure 3. ASTER VNIR subsystem. Along-track stereo geometry of ASTER band 3: backward (3B) and nadir (3N). Adopted from Graphic created by Dr. Andreas Kaeaeb, Department of Geography, University of Zurich, Switzerland.



ASTER data can be obtained from the USGS/Earth Resources Observation System (EROS) data center in several processing levels. Level 1 products contain data for all bands of the ASTER instrument. Higher-level data products such as DEM (level 3) are derived from level 1 data. Two types of Level 1 data products are offered depending on the degree the raw data is processed: Level 1A and Level 1B.

Level 1A is the preferred input data for the DEM extraction because the image data maintain the original data values at full resolution since the radiometric and geometric coefficients, supplied in the metadata, are not applied to it (Earth Remote Sensing Data Analysis Center [ERSDAC], 2002). Level 1B data has both the radiometric and geometric coefficients applied, therefore such data are less suitable for DEM extraction (van Ede, 2004).

### *ASTER DEM Acquisition*

ASTER DEMs can be acquired from the Land Processes DAAC at EROS Data Center as an on-demand product or can be processed from the stereopairs using proper software. Some of the common commercial software that include the algorithm for generating ASTER DEMs include the latest versions of ERDAS Imagine, ENVI and PCI Orthoengine. For the purpose of this study, the DEM was acquired from EROS Data Center.

Two types of DEM can be obtained from ASTER: Relative and Absolute. A relative DEM is generated by using only the satellite ephemeris data and therefore has a positional accuracy that depends upon the stability of the spacecraft and other factors.

An absolute DEM uses GCPs to more accurately geolocate the image and yields a product with real ground elevations. According to the product description in the ASTER User Handbook, with appropriate ground control, the horizontal and vertical accuracy of an absolute DEM can be up to 7 m. The Relative DEM is not nearly as accurate as the Absolute DEM horizontally since the Relative DEM is geo-coded using only satellite ephemeris data (ERSDAC, 2002).

The on-demand Absolute DEM supplied by LP-DAAC is geo-coded using client-supplied Ground Control Points. The client must first order the L1A data, locate the GCP's on both the 3N and 3B images and supply their pixel coordinates along with the GCP coordinate locations. A single 60 km x 60 km ASTER data granule (14 bands image) containing stereo data costs \$55 US, plus a \$5 US handling charge. The granule "SC:AST\_L1A.003:2017932815" produced on October 28, 2003, was found after a meticulous search of the EROS archive. The search was centered over a high concentration of landfills in the Bay Area, looking for a cloud-free image with high radiometric contrast.

### *Ground Control Points*

The accuracy of the Absolute DEM depends largely on the number and the distribution of the GCPs collected. According to Toutin (2002), only four precise GCPs are theoretically sufficient to obtain Absolute DEMs, but "the use of overabundant GCPs enables to avoid their error propagation in the modeling and to keep accuracy in the order of one pixel (15 m)." Also, in a study to evaluate DEMs from different satellite images,

Subramanian, Singh & Sudhakar (2003) point out that for creating a good DEM from ASTER, the GCPs must be well spread over the entire area, and most GCPs should be collected in low altitude areas and less on maximum elevation. “The reason being high altitude areas have lean and their image position does not reflect true ground position and hence X-Y references taken for such points results into large RMS error” (p. 10).

For that, 35 GCPs were collected and 24 were provided with the request for an Absolute DEM (Figure 4). GCPs that were not selected for DEM generation were used in the accuracy assessment of the DEMs.

#### *GCPs Selection*

Locating GCPs for ASTER DEM is a time consuming task that should be meticulously performed to obtain a good DEM. Each pixel reflecting a GCP should be located in both bands to be used as a tie point (TP) to correlate the nadir and back-looking bands. For this study, each GCP was located and documented before the field survey (see example in Figure 5). The process involved the following steps:

- Preview of ASTER stereo bands using Freeview V9.1 (from PCI Geomatics) and setting the coordinates to raster to obtain line and sample values of distinct GCPs on the imagery in both bands.
- Locate GCPs based on: distribution (as discussed earlier), consistency (features that do not vary with time), and resolution/contrast (the extent of the features and their contrast with the surrounding to be within 1 pixel in both bands).

- Find the real world location of each GCP using free Internet services such as GlobeXplorer.com, terraserver-usa.com, and Topzone.com. The address of each location was found by previewing high-resolution aerial photos and large-scale maps online.
- Plan field trips route and print documented maps and images for each GCP, with driving directions.

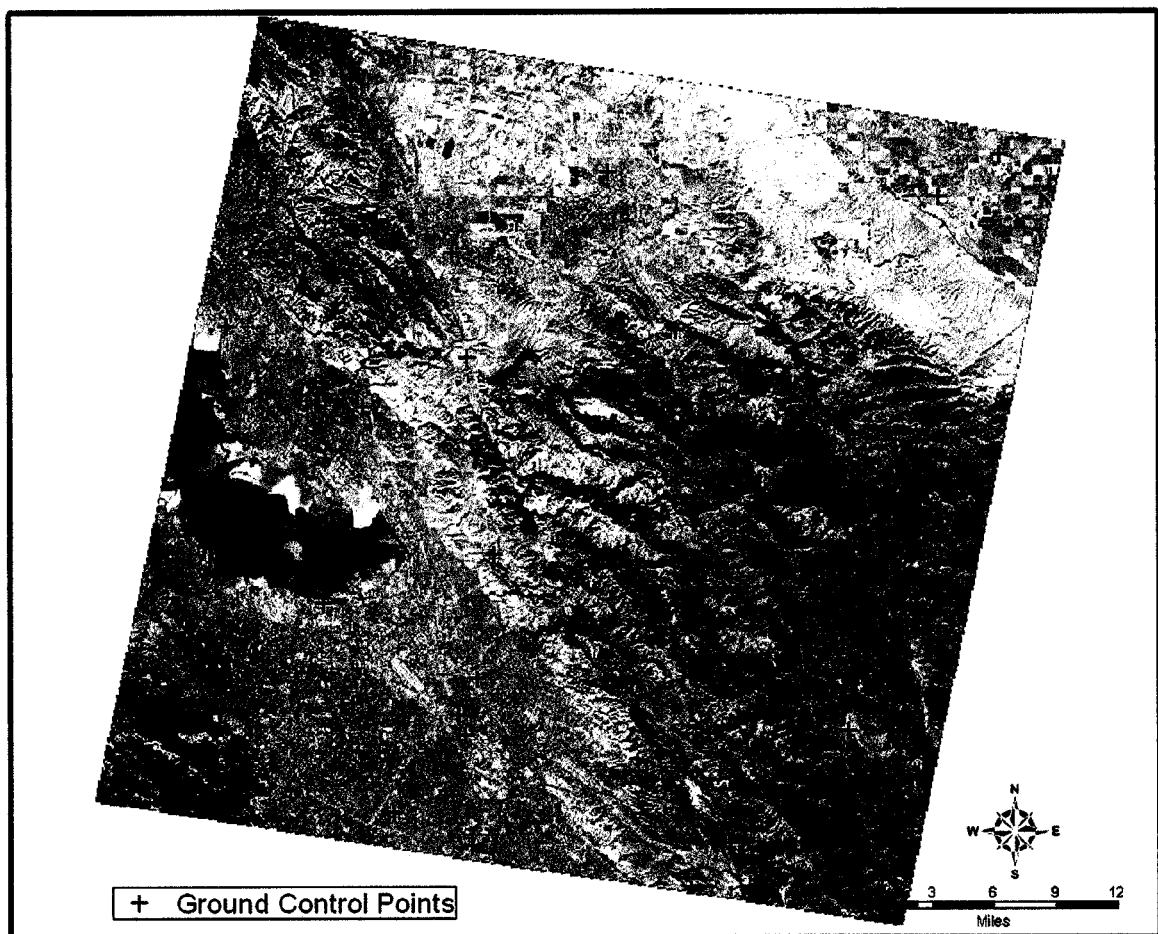


Figure 4. Distribution of ground control points used for ASTER DEM generation

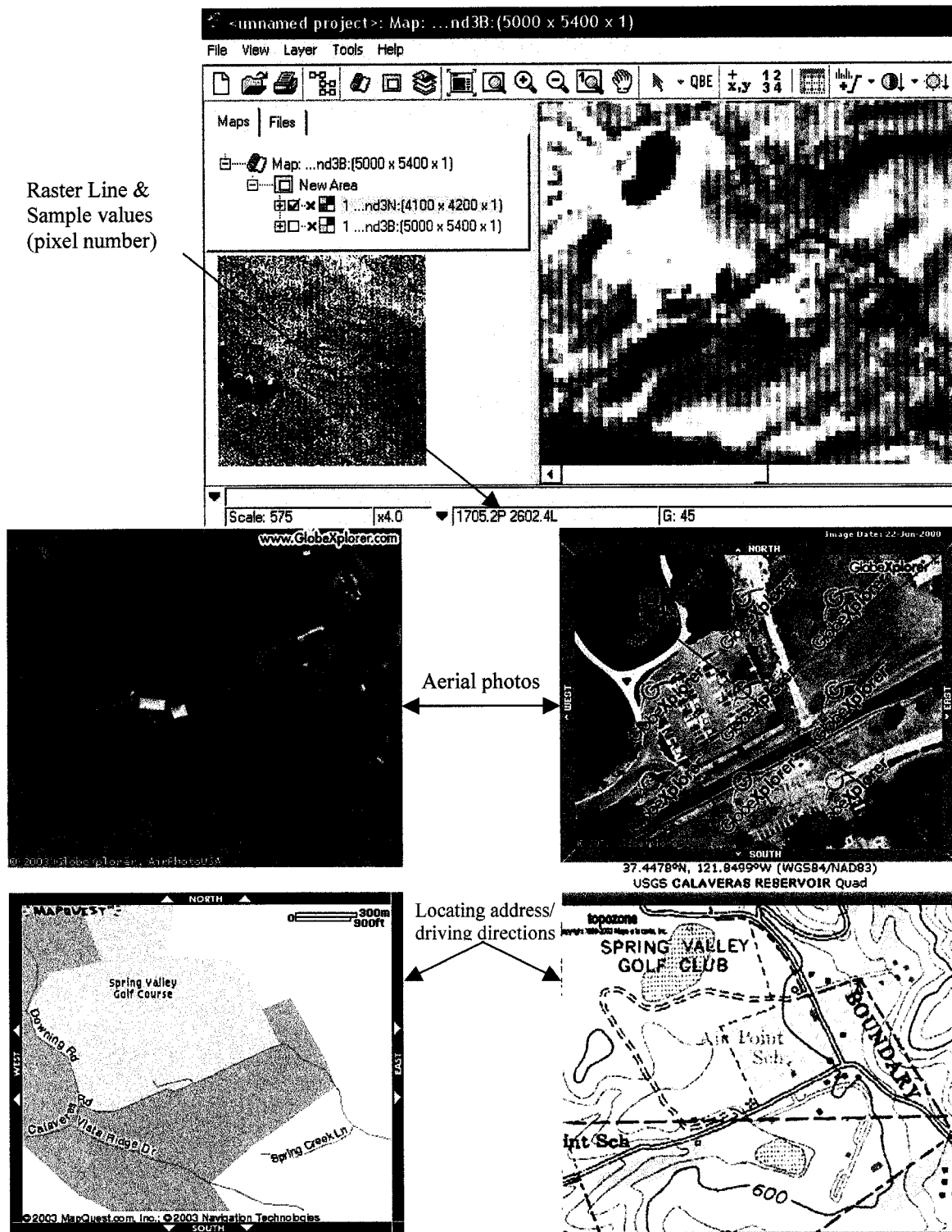


Figure 5. Locating distinct features on ASTER 3N and 3B bands using Freeview, and planning the GPS field survey.

## *GPS Survey*

Although the accuracy needed to reference an ASTER image is more or less 5m (Vogt & Arigony, 2002), achieving an accuracy of  $\pm 1$  meter was essential in order to discount GPS measurement errors from the total error variance between DEMs in the analysis. GPS measurements were performed using a handheld Trimble Geoexplorer III. The GPS receiver was configured for high precision (See Appendix A). GCP descriptions were entered in the data dictionary of the GPS before the survey. Each GCP survey consisted of multiple log measurements (50 to 120) gathered in one log file in 4 to 10min. During the field survey, more information were appended to the GCPs metadata such as sketches, marking the exact pixel on the images where the measurement was taken, and the date & time.

“Data collected by GPS receivers is subject to errors, including small satellite clock errors and larger errors intentionally introduced into the system by the US Department of Defense. The vast majority of these errors can be removed from the data by differential correction” (Trimble Navigation Limited, 1999). Therefore, post-processed real-time differential GPS correction was applied to the collected data in order to eliminate error. This involved using the Trimble’s Pathfinder Office software to compare GPS data to data collected by base stations near the GCPs, at the exact same time. The Pathfinder also averages the multiple position measures taken for each GCP.

The final GCP coordinates (lat/long and elevation) and their corresponding pixel number (line and sample) in each of the stereo bands were dispatched to the LP-DAAC to generate the Absolute DEM (see Appendix B).

#### USGS 7.5 minute DEM

The DEM data for 7.5-minute units correspond to the USGS 7.5-minute topographic quadrangle map series for all of the United States and its territories except Alaska. The data are produced in 7.5- by 7.5-minute blocks from either digitized cartographic map contour overlays or a scanned National Aerial Photography Program (NAPP) photographs. The DEM data are stored as profiles with a 10- or 30-meter square grid spacing along and between each profile (USGS, 2004).

The accuracy of DEM data depends on the source and resolution of the data samples. DEM data accuracy is derived by comparing linearly interpolated elevations in the DEM with corresponding map location elevations and computing the statistical standard deviation or root-mean-square error (RMSE). The RMSE is then used to describe the DEM accuracy. For 7.5-minute DEM's derived from a photogrammetric source, 90 percent have a vertical accuracy of 7-meter RMSE or better and 10 percent are in the 8- to 15-meter range. For 7.5- minute DEM's derived from vector or DLG hypsographic and hydrographic source data, an RMSE of one-half of a contour interval or better is required (USGS, 2000, Data Accuracy section).

### *7.5 minute DEM Acquisition*

The original DEM 7.5 minute tiled data is available in Spatial Data Transfer Standard (SDTS) form. It can be obtained at no cost from the Internet. For this study, it was downloaded from GeoComm International Corporation at <http://gisdatadepot.com/dem>. Although the data were free, gathering it was not an easy task. Since the data is in 7.5- by 7.5-minute blocks, 42 tiled transfers were necessary to encompass the area covered by the ASTER DEM. Searching the database by county, each transfer had to be downloaded separately. An SDTS transfer is composed of multiple files combined into one physical file with the tar utility, and then compressed (e.g., 1663840.DEM.SDTS.TAR.GZ for San Jose West quad).

### *SDTS Import and DEM Mosaicking*

The SDTS data were previewed using Freeview Ver. 9.1 from PCI Geomatics to pinpoint the needed quads (also called 7.5' DEM blocks or tiles). Using ERDAS Imagine V8.5 the tiles were imported into individual raster grids (\*.img extension).

One of the odd characteristics of the 7.5' DEMs is the random change in vertical units between meters and feet from one tile to another. Therefore, the tiles with elevation units in foot were converted to meters using the "DEM Height Converter function" in ERDAS (1m = 3.28084 ft).

Then, using the mosaic tool in ERDAS, the tiles were joined to form one larger DEM. Not all settings for the mosaic application were left to default because elevation



data on each quad neatlines (all four sides) share edge profiles with the surrounding quadrangles. Two default settings had to be changed:

- The grid sampling density was set to 4 pixels instead of the default 16. Using higher sampling density caused noticeable edge breaks between quads because the neatlines were skipped.
- The overlap function, which is the method for stitching the two images together along common quad edges, was set to “Maximum.” Neatline values are usually set to -32,766 (void areas) in a way to interlock with the values of the adjacent quad. Changing the setting to “Maximum” insures that the value of each pixel in the overlap area is replaced by the greater value of the corresponding pixels in the overlapping images.

### National Elevation Dataset (NED)

The USGS National Elevation Dataset (NED) is a raster product assembled by the US Geological Survey in an effort to deliver a seamless DEM coverage of the United States, Hawaii, Alaska, and the island territories. The NED was developed and is being updated bi-monthly by merging the highest-resolution, best quality elevation data available. NED has a consistent projection, resolution (1 arc second  $\approx$  30m), and elevation units (meters). The horizontal datum is NAD83, except for Alaska (AK), which is NAD27. The vertical datum is NAVD88, except for AK, which is NAVD29. A 1/3 arc second (10m) NED is also being developed as higher resolution data covers the US.

NED data sources are selected by priority from available DEMs. The highest priority goes to high-resolution elevation data derived from photogrammetric mapping and from Lidar data, followed by the USGS DEMs 10-meter grid, the 30-meter Level 2 grid, the 30-meter Level 1 grid, the 2-arc-second resolution for Alaska, and the 3-arc-second resolution that is used only to fill in values over some large water bodies. The sources date from 1925 to 1999.

As with the 7.5-minute elevation data, NED accuracy is set to  $\leq 7\text{m}$  RMSE. During the NED assembly process, artifacts that are commonly found in older DEM's have been filtered to improve the quality of the information that can be derived from it such as slope, shaded-relief, and drainage and watershed simulations (USGS, 2003).

The NED can be obtained for free from the Internet using the Seamless Data Distribution System (SDDS) developed by USGS/EROS data center. The SDDS enables a user to view and download US seamless data using an interactive map. The user can use the interactive method to select a rectangular area to download or can define the desired area by coordinates. The NED for the area of study was downloaded in ArcGRID format, which can be directly read by ERDAS IMAGINE and ArcGIS.

## DATA PREPARATION FOR INSPECTION AND ANALYSIS

Since the acquired DEMs had different projections and resolution (see Table 1 below), they had to be standardized before assessing their quality and comparing them. Although the North American Datum of 1983 (NAD83) is the preferred projection for the US area, adopting it required resampling the NED file to 30m spacing in addition to reprojecting ASTER and the 7.5' DEMs. To minimize spatial shift errors induced during transformation processes (geometric rectifications), the USGS DEMs were instead reprojected/resampled to ASTER DEM specifications: Universal Transverse Mercator (UTM) coordinate system referenced to the World Geodetic System of 1984 (WGS84), with 30m resolution. This was done using the “geometric correction | reproject” function in ERDAS Imagine. Then, the USGS DEMs were subsetting to the same area coverage of ASTER DEM.

Table 1. Acquired DEMs original projection and resolution

DEM	Projection	Spheroid	Datum	Resolution
ASTER	UTM	WGS84	WGS84	30 m
7.5 minute	UTM	Clarke 1866	NAD27	30 m
NED	Geographic (lat,long)	GRS 1980	NAD83	1 arc second ( $\approx$ 30 m)

## DATA INSPECTION AND QUALITY ASSESSMENT -

### EXPLORING THE DEMS

#### Comparison of DEM Data with High Accuracy Control Points

After standardizing the data, all three DEM products were evaluated for vertical accuracy by comparing them to 76 control points: 65 were derived from 1:24/25K USGS topographic maps using the online service Topozone ([www.topozone.com](http://www.topozone.com)); 11 of them were acquired as part of the GPS survey. Several studies marked problems in ASTER DEM accuracy for steep terrain due to some model distortion (discussed later), therefore the selected control points were located on flat terrain at different altitudes to assess the stereo model stability and avoid measuring elevation errors that stem from model flaws in ASTER data.

DEM Accuracy is expressed in terms of RMSE or Root Mean Square Error. “The RMSE statistic is essentially a standard deviation and is thus based on the assumption that errors in the DEM are random and normally distributed” (Wechsler, 2000). To facilitate the task of examining elevation values in each DEM at each control point, the three DEMs were combined into a three-band image using the “Image interpreter | utilities | layer stack.” Then the spectral profiler was used to output the elevation values in all three DEMs simultaneously.

The elevation root mean square error (RMSEz) was computed in Excel. RMSE is

expressed as:  $\sqrt{\frac{\sum_{i=1}^N (y_i - y_j)^2}{N - 1}}$ , where:

$y_i$  is an elevation from the DEM  
 $y_j$  is the "true" known or measured elevation of a test point  
 $N$  is the number of sample points.

According to the USGS DEM standards, the maximum absolute elevation error permitted should not exceed three times the RMSE desired accuracy. The result in Table 2 show that the USGS DEMs met the standards even after resampling. The ASTER DEM results were remarkable, with a vertical RMSE < 10 meters and a maximum error less than 2 times the standard deviation. Note that these results do not reflect elevation errors in rugged terrain resulting from georeferencing warp.

Table 2. Statistical results: root mean square (RMS) and maximum elevation errors of the DEMs computed with 76 control points.

	National Elevation Dataset	USGS 7.5minute DEM	ASTER Absolute DEM
RMSEz (m)	2.63	2.92	9.58
Max Difference (m)	5.18	5.83	18.94

### Flaws in ASTER Absolute DEM

Typically, LP-DAAC assigns negative values for the background (-150) and failed areas (-100) of ASTER DEMs. However, displaying the received product in 3D view revealed unrealistic elevations in water bodies (Figure 7), and irregular negative

coastal values (Figure 6). According to Toutin (2002), snowfields, lakes, and shadowed/occluded areas may cause failure or generate artificial relief during the correlation process when generating ASTER DEM. Furthermore, his study revealed that in rugged topography the accuracy decreases with steeper terrain with an “almost-linear correlation: stronger is the slope worse is the elevation accuracy.” In this case, vertical errors may stem, to a great extent, from planimetric errors, where the difference in elevation ( $\Delta z$ ) is in part due to relief mismatch ( $\Delta xy$ ) that stems from the model distortion (shown in Figure 6).

To further inspect the DEM, a three-band natural color image was created from the L1A VNIR bands: 1, 2 & 3N and geocoded in ERDAS for visual interpretation and transect profiling. As shown in Figures 6 and 7, both the natural color image and the DEM Layers stack were opened in ERDAS software in separate viewers and linked geographically. ERDAS spatial profile tool allows the display of the desired transects in both viewers simultaneously which helps recognize the features of the surface being profiled. Peculiar elevations in the DEM proved to be areas of constant tone as stated above (water bodies, etc.).

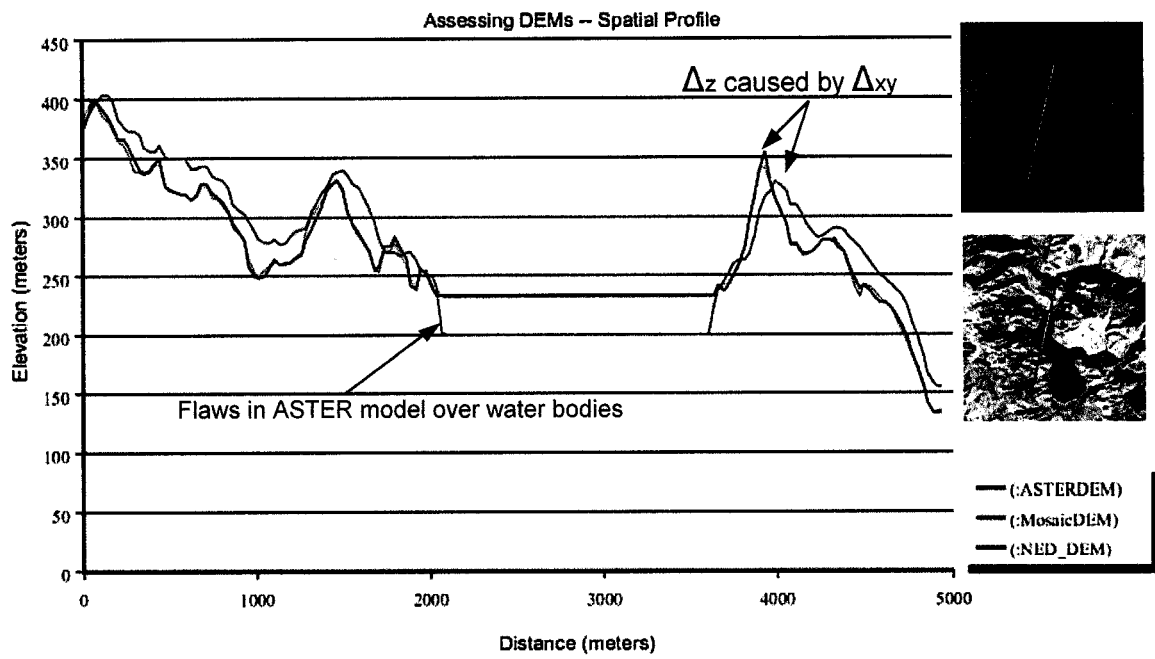


Figure 6. Transect profile over Calaveras reservoir and surrounding area

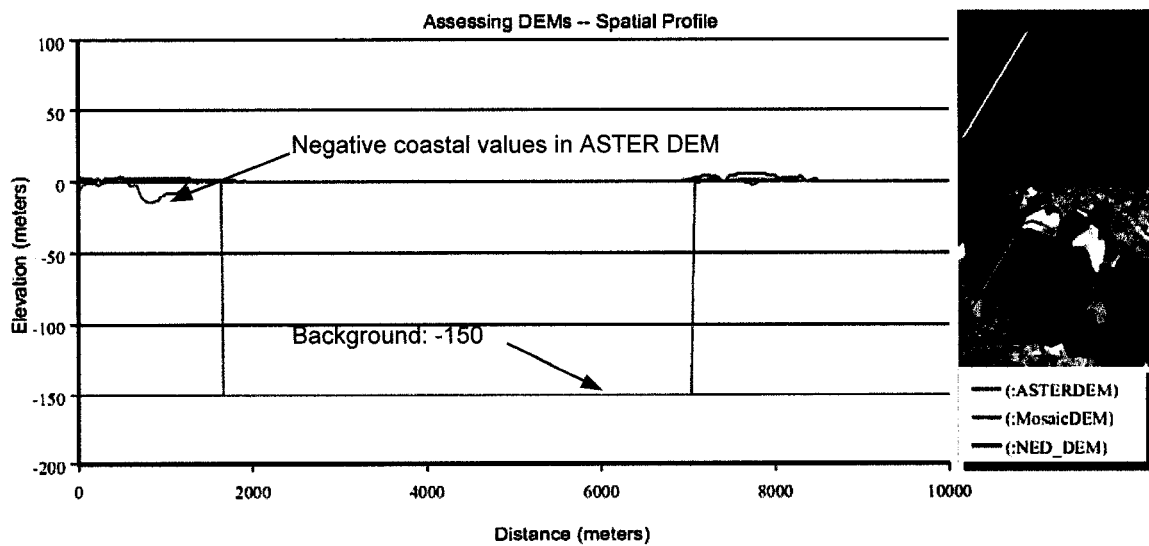


Figure 7. Transect profile over San Francisco Bay, from East Palo Alto to Newark city

## ELEVATION CHANGE DETECTION APPROACH

Simply put, the comparison of two DEMs, with similar specifications, surveyed at different dates over the same area, should reveal any elevation change that might have occurred during that time difference, when the change meet the following:

1. The difference in elevation ( $\Delta z$ ) is higher than the combined maximum possible error of each DEM.
2. The change occurs over an area larger than the spatial resolution of the DEM + the horizontal error ( $\Delta xy$ ).

DEMs are simply compared by deducting one from another. Since ASTER DEM layer include background values (-150), the following function was created in the spatial modeler to compare both the USGS 7.5' DEM mosaic and the NED with the complete ASTER DEM on a pixel by pixel basis:

```
CONDITIONAL {(ASTER_DEM == -150) -500 , (ASTER_DEM >= 0) ROUND  
(ASTER_DEM - $n10_PROMPT_USER)}
```

The above expression states the following: if the cell value on ASTER DEM layer equals -150 (background value) then assign -500 to it; otherwise, subtract ASTER DEM layer from a user-selected layer to the nearest integer (ROUND). The background value in ERDAS must be a numeric constant, which is why a unique value (-500) was assigned to it.



## Statistical Assessment of the Variance between ASTER and USGS DEMs

The new raster resulting from the above function carries the difference in elevation values between two DEMs at each pixel; alias “Variance Raster” (VR). For the analysis, the VR files were imported into ArcMap software because of its ease in multiple data display and in classification capabilities. Using the raster calculator from the Spatial Analyst extension, the background value was assigned a value of “nodata” using the SetNull function, and the new raster outputs were further analyzed statistically for mean, min, max, standard deviation, and level of agreement. The Histogram plot of the VR illustrating a bell shape in Figure 8 indicates that differences between the DEMs are random and normally distributed with mean and standard deviations of about 5m and 15m respectively (Table 3).

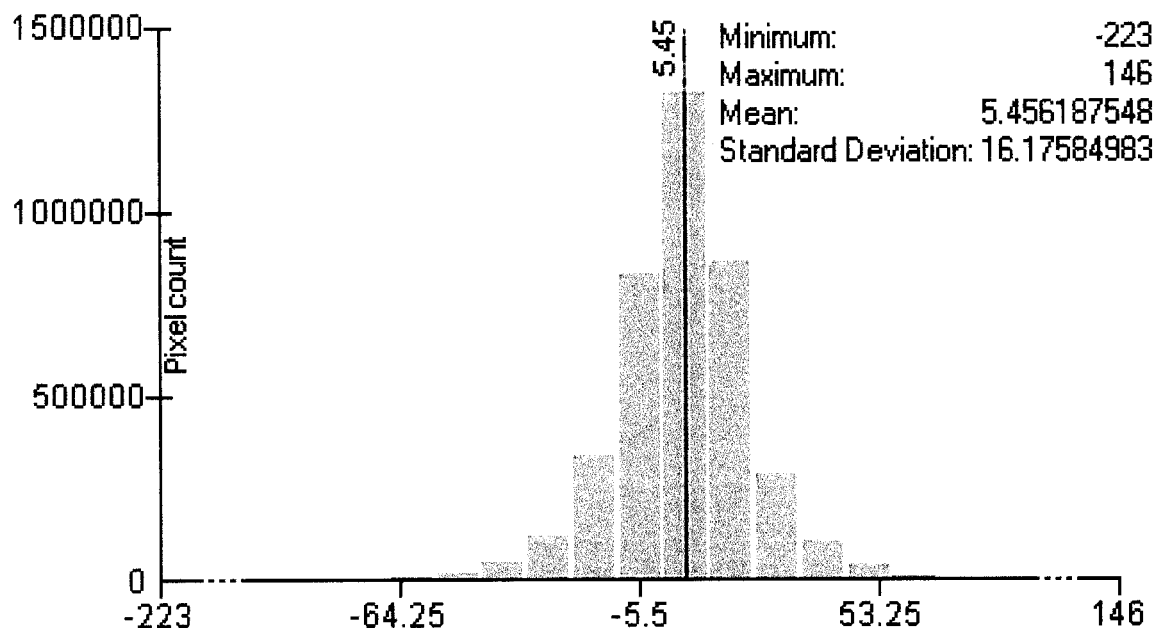


Figure 8. Histogram analysis showing a normal distribution in elevation differences when comparing every pixel of ASTER DEM with that of a USGS 7.5' raster.

The results of the statistical analysis in Table 3 show that although the values of ASTER DEM are closer to the NED than the USGS 7.5' DEM, the variance between the ASTER DEM and the USGS 7.5' DEM is roughly identical to that of the NED.

Furthermore, 75% of ASTER DEM values fell roughly within 15 meters (approximately one standard deviation [ $\delta$ ]) of those of USGS elevation models, 95% within  $2\delta$ , and 99% within  $3\delta$ , which indicates that the elevation model is stable considering that the elevation differences are in part the result of pixel location mismatch stemming from:

- Comparing different types of DEM developed by using different methods.
- Raster warping when reprojecting the USGS DEMs.

Table 3. Statistical results (in meters) of elevation differences between the ASTER-extracted DEM and the USGS DEMs.

$\Delta z$ in meters	within absolute				Mean	Min.	Max.	Standard Deviation
	7m	15m	30m	50m				
<b>ASTER /USGS 7.5'</b>	43%	74%	95%	99%	5.5	-223	146	16.2
<b>ASTER/NED</b>	43%	75%	96%	99%	4.6	-218	139	13.5

#### Temporal Elevation Change Detection -- Visual Inspection

Color and contrast are two important factors for distinguishing discrepancies by visual inspection. At first, when the VR files were opened in gray scale without histogram stretch, minimum and maximum values could not be easily distinguished from

the rest of the data. Therefore, multiple approaches of image enhancement were tested to improve the visual interpretation of the data at hand. Hotspots were immediately detected in the VRs using the histogram stretch (min-max) and drawing the stretched data values along a color ramp (Figure 9). Additional enhancements were applied to improve the contrast in suspect areas. Calculating the natural logarithm ( $\ln$ , base  $e$ ) of the VR and classifying it proved to be an efficient method as well (Figure 10); the logarithm function separates the data into classes by stretching low values and condensing higher values (for example:  $\ln 5 = 1.6$ ,  $\ln 10 = 2.3$ ,  $\ln 50 = 3.9$ ,  $\ln 100 = 4.6$ ). The enhanced variance raster images were inspected at different scales (zoom), and 1:100,000 proved to be the overall preferred scale for scanning.

The hotspots (suspect areas) found in the VR ASTER-7.5' matched the ones detected in the VR ASTER-NED. Since the 7.5-minute elevation data for the conterminous United States are the primary initial data source for the NED, this result was expected but needed confirmation.

Looking at the full VR images in Figures 8 and 9, and knowing that these values reflect positive and negative differences (ASTER - USGS DEMs), the following could be discerned:

- The values of ASTER DEM are higher than the compared USGS DEMs in the middle of the scene than on the edges, with the exception of the southwest corner.
- The distinction between mountainous areas with steep terrain, where colors are jagged, and flat terrain where variation is mild and smooth is apparent.

- Some areas show extreme contrast with their surrounding, and are large enough to be suspected for possible temporal elevation change.
- Water bodies such as lakes and ponds have significantly lower values than the actual elevation - a known systematic flaw in ASTER data.

Additional analysis performed on the data in ArcMap confirmed that in regions where slope < 5 degrees, over 96% of the VR values fall within one standard variation. This means that the level of agreement of ASTER DEM with DEMs from the USGS is more than 96% in flat terrains. Therefore, lower variation values (20 to 30 m) in those areas triggered suspicion.

Suspect areas were thoroughly examined by:

- Inspecting the differential range and checking the original values in the source DEMs for credibility.
- Checking the history of the corresponding 7.5' DEM quad (creation date and source date).
- Visually inspecting aerial photos and topographic maps using online services: [www.terraserver-usa.com](http://www.terraserver-usa.com), [www.topozone.com](http://www.topozone.com), and [imageatlas.globexplorer.com](http://imageatlas.globexplorer.com).
- Investigating present and historical activities in areas where temporal elevation change has almost certainly occurred.

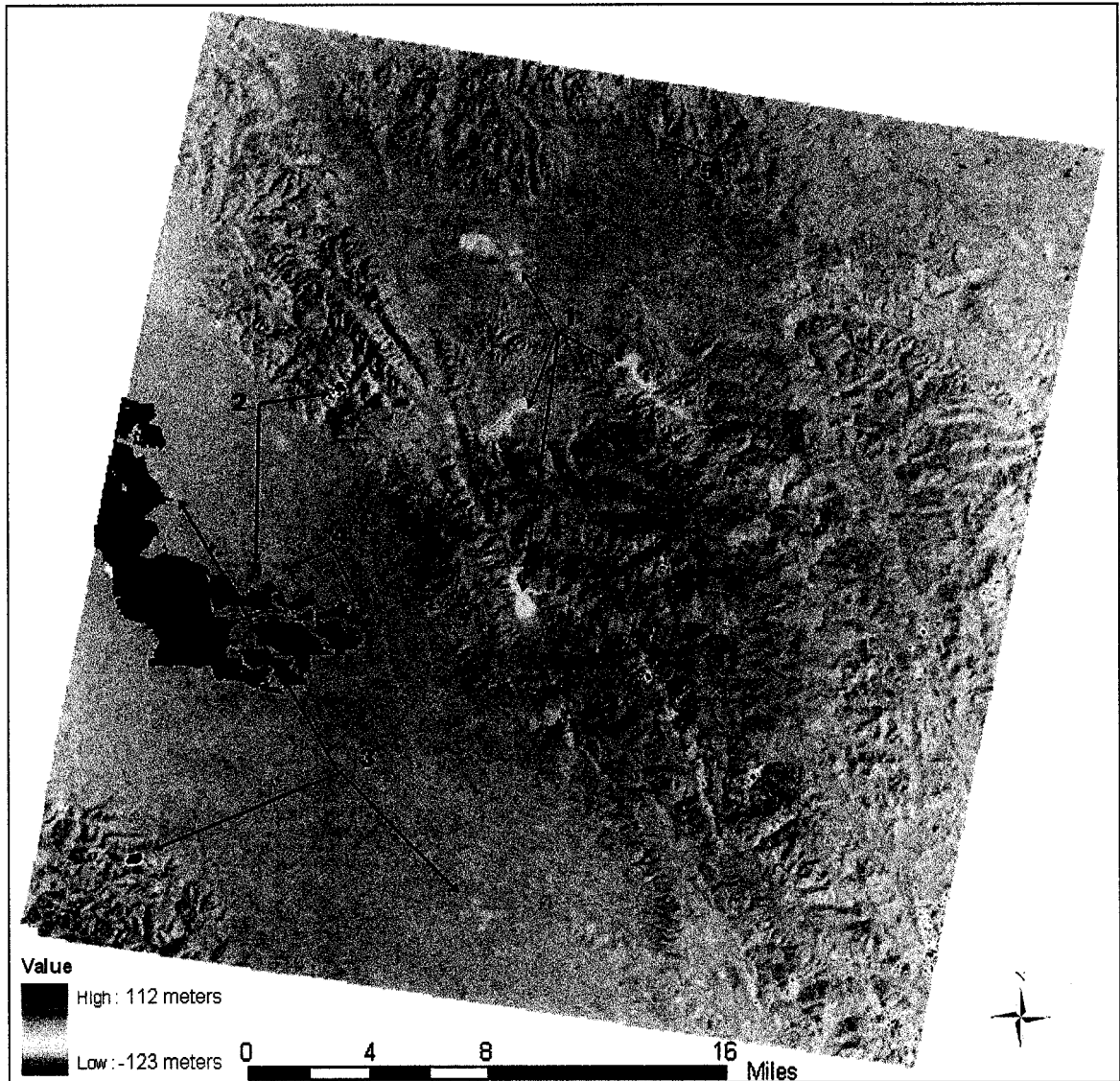


Figure 9. Min-max histogram stretch of the variance raster between ASTER and the 7.5' elevation mosaic (VR ASTER-7.5').

- 1: Lakes and ponds
- 2: Protrusion of major variances due to data flaws in ASTER data
- 3: Quarries and mines detection.
- 4-5: Landfills detection

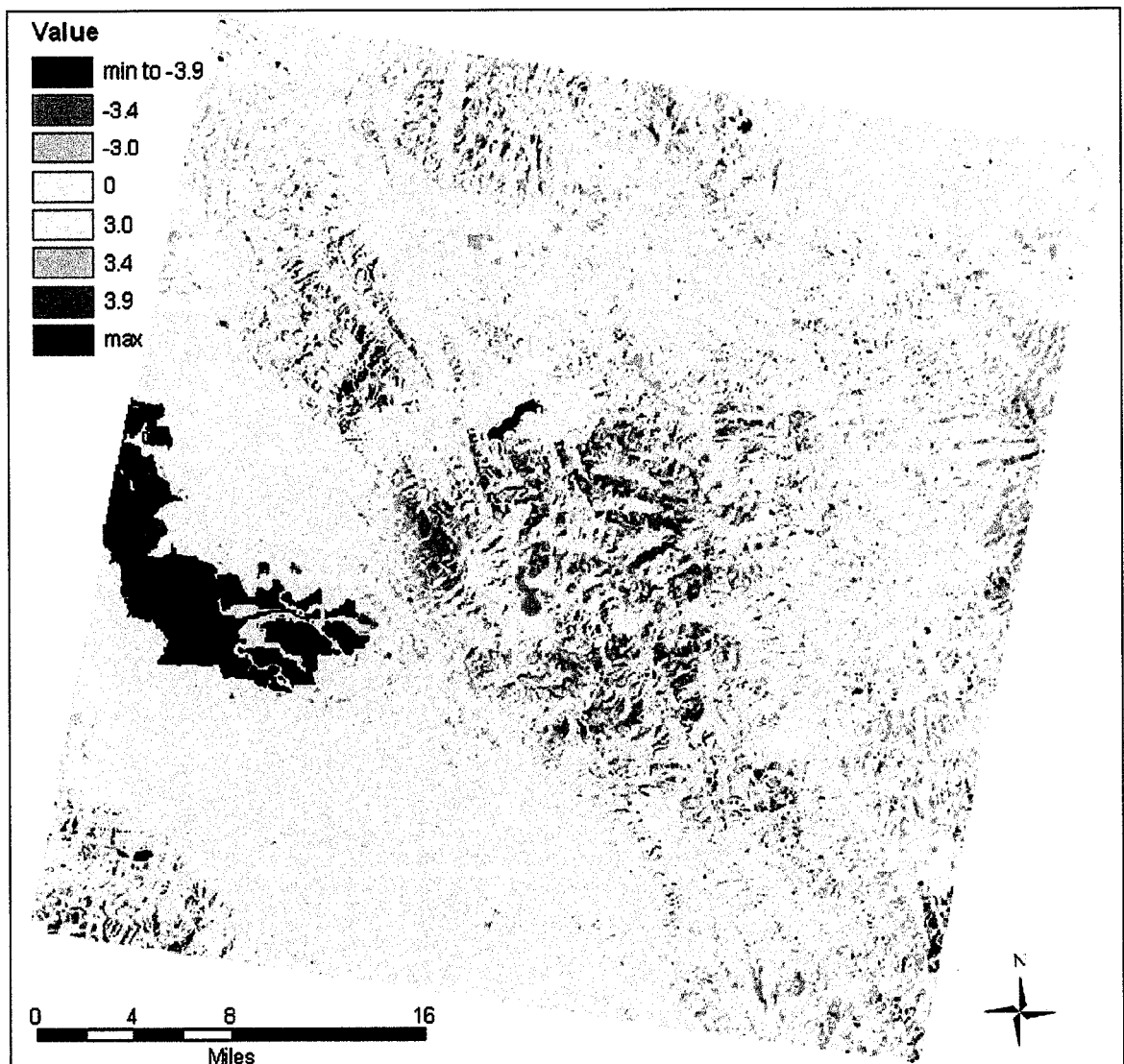


Figure 10. Classification of the natural logarithm of VR ASTER-NED. The same suspect areas found with min-max histogram stretch could be distinguished, but with better contrast.

## RESULTS AND DISCUSSION

Differences in elevation between the DEMs could be due to one or a combination of the following:

- 1- False difference related to products accuracy
- 2- True difference from land cover
- 3- True difference from temporal changes

### False Difference Deriving from Products Accuracy

The variance between the DEM extracted from ASTER data and the USGS DEMs is mostly due to errors present in both products, mainly ASTER DEM. These errors are attributed to vertical accuracy (elevation) and to circular accuracy (horizontal). When data is reprojected from one coordinate system to another, spatial warping occurs, which increases circular error. The latter is especially significant in hilly topography because pixel location mismatches produce additional errors when comparing two DEM sources. In addition, ASTER DEM data contain large vertical errors that occur mainly in mountain ridges and slopes, and in lakes. Other significant errors throughout the scene occurred in areas that shared similar spectral characteristics such as saturation (high reflectance) and same intensity level (constant tones). These flaws in ASTER data seem to be systematic and product specific. Major differences resulting from systematic errors were recognized from their pattern during visual inspection. In some cases, extreme elevation differences over sizeable areas were suspected for temporal change but further inspections proved that they were only blunders (see Figure 9, #2).

### True Difference from Land Cover

The ASTER DEM is an optically based product. The elevation values reflect the land cover, including forests canopies, and the top of urban developments. Elevation values from the USGS DEMs (7.5' and NED) is a bare ground reading that reflects the landscape. Therefore, elevation differences detected in forests and urban areas stem in part from the land cover. Although irrelevant for many scientific applications, the detection of elevation differences from land cover is noteworthy for the purpose of this study because it indicates the potential of ASTER DEM data despite its flaws. Some major differences that protruded from their surrounding proved to be large urban developments or big constructions such as the Naval Air Station hangars in Figure 11-A.

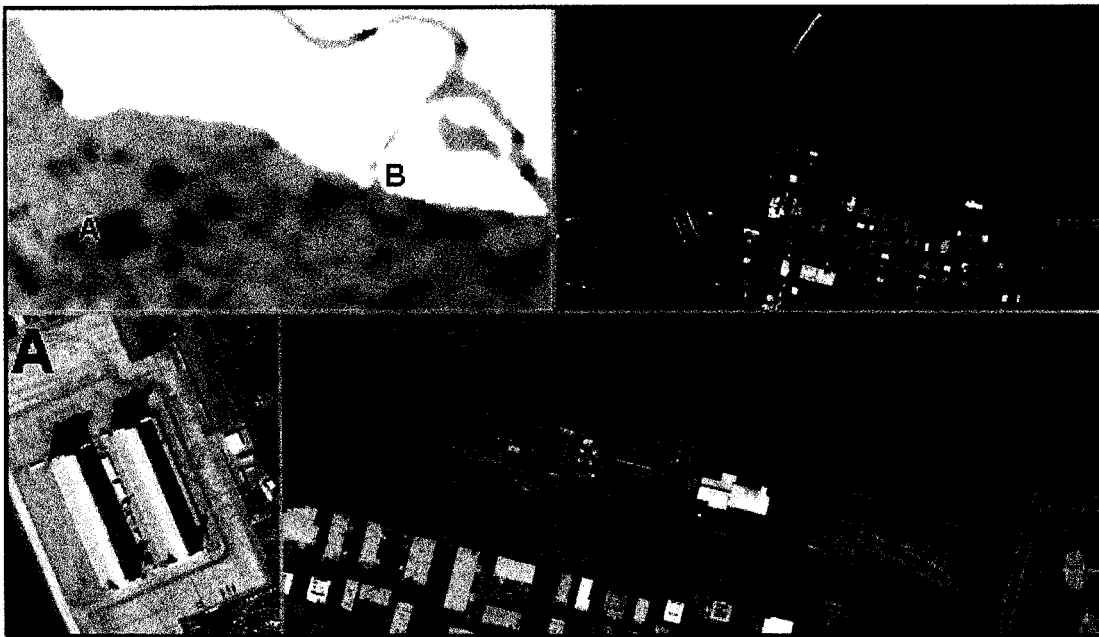


Figure 11. Land cover elevation difference detection  
A: Air Station hangars.  
B: Smart station - solid waste landfill and recycling facility.



### True Difference from Temporal Changes

Theoretically, major temporal topographic changes from natural or human causes (flooding, landslides, landfills, quarries, major development projects) should be detectable by comparing the two DEMs as long as the elevation difference for the same location is higher than the margins of circular and vertical data error. Since ASTER DEM accuracy is higher in flat terrain, elevation differences in the order of 20m ( $\approx 1.5 \delta$ ) or higher were considered significant enough to carry out an inspection in these parts. Because of the known flaws in ASTER DEM in hilly topography, the elevation threshold in these areas was set to 50m ( $>3\delta$ ). In addition, during the visual verification of the enhanced VR images side-by-side with the natural color image, perceivable though non-measurable thresholds were applied to the size and shape of areas with major elevation differences, such as the ridge and water lines patterns found in steep terrain.

Unquestionable temporal elevation changes were detected in nearly all of the most suspected areas. The detected changes were all the result of human impact/activities (Table 4). Changes in elevations from natural causes (e.g., landslides) were not detected although known to exist in the area. Some of the detected areas were already marked as disturbed surfaces (e.g., quarries and mines) on the USGS outdated topographic maps. The contours levels on those maps matched the USGS DEMs values.

The first five identified locations in Table 4 (bold font) are typical cases of surface change detection in this study. They represent relief drop (quarries) and rise

(landfills) detected in both flat and hilly areas (Figures 12 to 15). The Hanson quarry case is the most remarkable and therefore will be thoroughly discussed.

Formerly known as the Kaiser Permanente Cement Plant, the Hanson quarry stretches more than two miles over the Cupertino Mountains, scarring more than 1400 hectares (3,500 acres) of the hillside. The ASTER DEM exhibits higher elevation in the western section of the quarry that is being used as a stocking area; the middle section is where the excavation has caused a large pit with a bottom elevation value depicted by ASTER to be >200 meters lower than the original relief. The eastern section is where the processing plant is located (Figure 12). The quarry is known to be in violation of a ridgeline easement agreement and for causing landslides onto public property. Run-off created by the quarry operations carrying excavation silt are also potential hazards for the downhill creeks, habitats and reservoirs (Couperus & Schmidt, 2004).

Landfills on the other hand (Figures 13 and 15), show a rise in the relief and the creation of new hills. The location and the elevations reached by the landfills are important in studies related to pollution and contamination hazards, scenic views (e.g., line of sight from residential and touristic areas), and even microclimate impacts.

What is very significant for this study is the fact that the USGS elevation models cannot be used for watershed or flood analysis in and around the disturbed areas found in this study.

Table 4. Location of temporal elevation changes detected and identified

	<b>Latitude</b>	<b>Longitude</b>	<b>USGS Quad</b>	<b>Source Date*</b>
<b>Hanson Quarry</b>	37.320	-122.112	Cupertino	1948
<b>Vasco Road Sanitary Landfill</b>	37.753	-121.723	Byron Hot Springs	1953
<b>Altamont Landfill</b>	37.750	-121.657	Byron Hot Springs	1953
<b>Coyote Hills Quarries</b>	37.538	-122.078	Newark	1997
<b>Newby Island Sanitary Landfill</b>	37.460	-121.943	Milpitas	1948
Santa Claire Landfill	37.425	-121.976	Milpitas	1948
Nine Par Landfill	37.435	-121.949	Milpitas	1948
Major residential Development	37.400	-121.880	Milpitas	1948
Palo Alto Refuse disposal site	37.45	-122.105	Mountain View	1997
NASA Moffett Field Landfill	37.43	-122.050	Mountain View	1997
Stierlin Rd Disposal AKA Ferrari	37.426	-122.073	Mountain View	1997
Smart station: Solid waste landfill	37.417	-122.008	Mountain View	1997
Hillsdale mine	37.289	-121.856	San Jose East	1978
Tri Cities Disposal Facility	37.500	-121.982	Niles	1948
Pleasanton Waste Disposal Site	37.664	-121.846	Livermore	1960
Hayward Quarry 1	37.639	-122.041	Hayward	1993
Hayward Quarry 2	37.664	-122.067	Hayward	1993
Major residential Development	37.750	-121.90	Diablo	1949

\* Indicates the source date of the elevation data not the creation date. For this study area the 7.5' DEM was created mid 1998, the NED was created from mid 1999 to mid 2000.

*Note: The first five cases marked in bold are illustrated in Figures 11 to 14.*

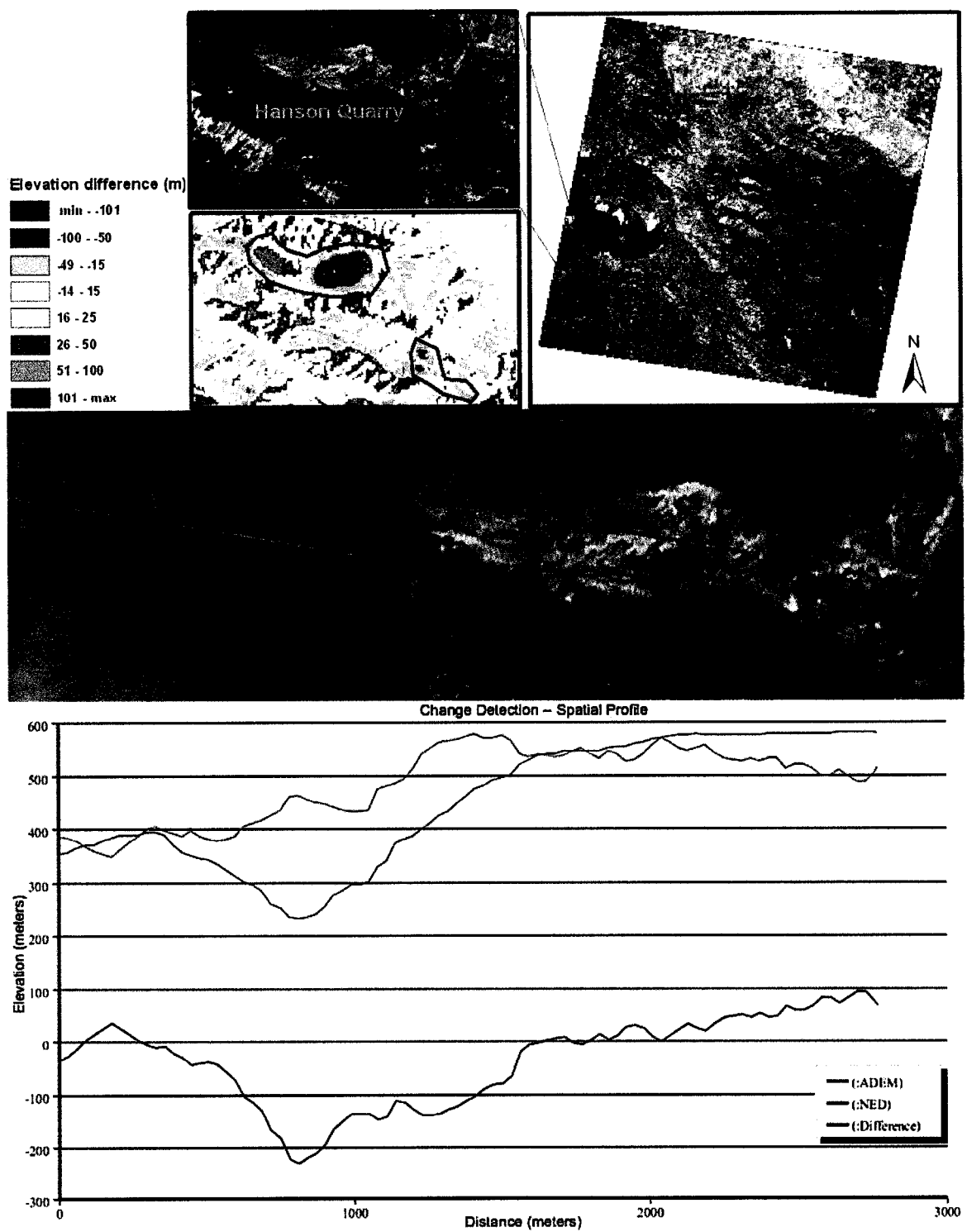


Figure 12. Hanson quarry detection and elevation change assessment.

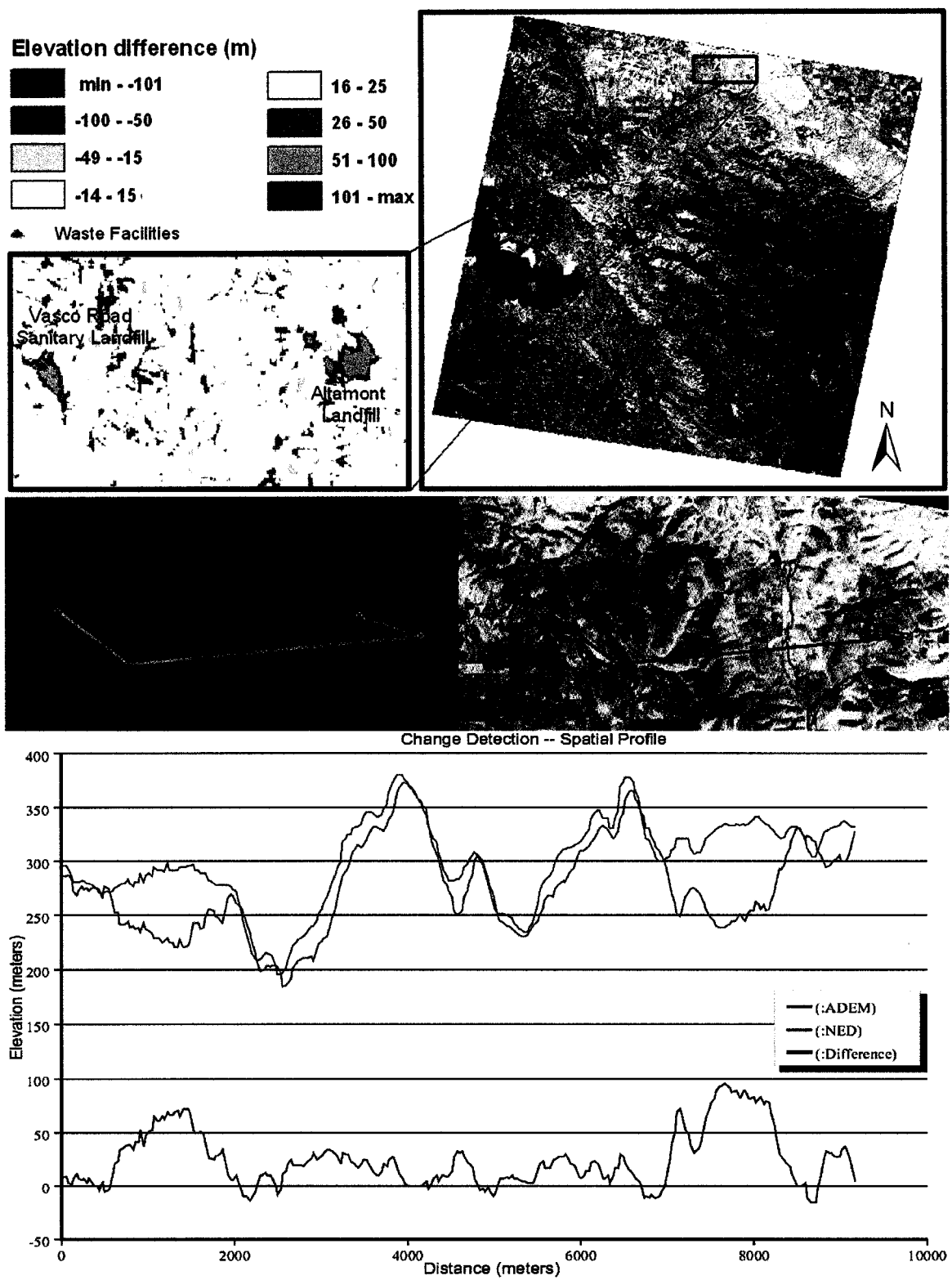


Figure 13. Landfills detection and relief change evaluation in Byron Hot Springs quad.

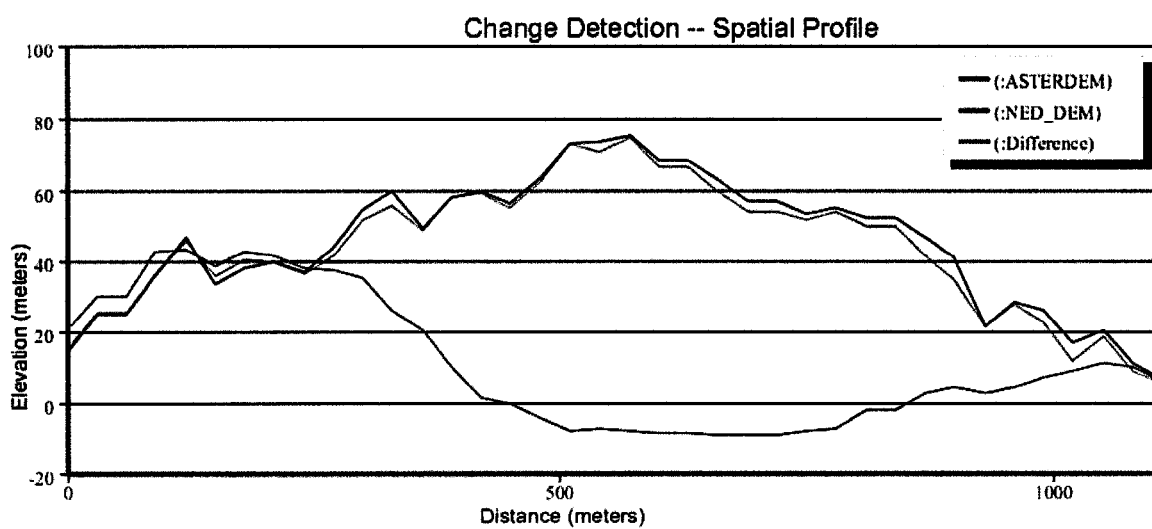


Figure 14. Coyote Hills Quarry detection on the coast, in Newark quad.

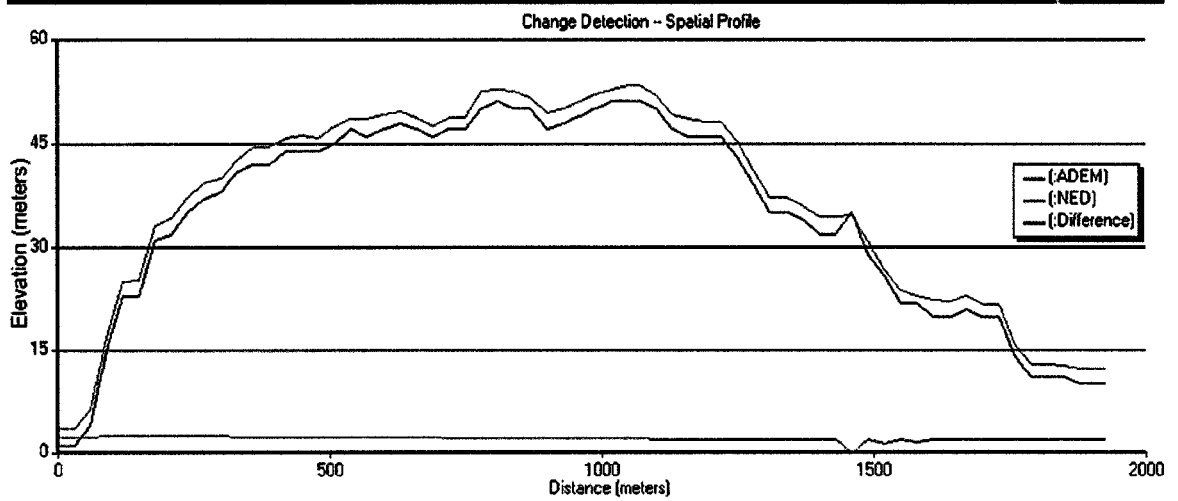


Figure 15. Newby Island Sanitary Landfill, Milpitas quad.

## CONCLUSION

The results of this study seem positively conclusive regarding the use of ASTER DEM to detect temporal elevation changes by comparing it to USGS elevation sources, but some reservations do apply. While the NED is the most recent and frequently updated elevation data distributed at no cost, comparing it to ASTER DEM revealed significant elevation-value mismatches beyond the margins of error in some localities that turned out to be areas disturbed by humans.

Human activities are changing the Earth's relief, and some of these changes are sizeable enough to consider analyzing their hazardous impact on human lives, the environment, and the economy. Earth surface change could also be caused by natural events such as volcano, earthquakes, landslides or deposition and erosion due to the topographic relief, precipitation, and soil and rock types. Finding such temporal elevation changes seem to be beyond the accuracy that can be obtained from ASTER DEM or even from the USGS elevation models. Such natural events usually take place in hilly relief where ASTER DEM accuracy deteriorates due to flaws in the system and/or the model. Also, since cross-registering different types of DEMs cannot be accurately performed, positional shifts in the data (increased when applying geometric transformations) induce unrealistic change detections in rugged terrain resulting from relief mismatch between the compared DEMs. Because of these limitations originating from data accuracy, not all kinds of surface changes that may have occurred could be distinguished, but the magnitude of the changes that were detected in this study are



substantial enough to deteriorate the quality of spatial analysis in research applications if not considered.

When acquiring elevation data, many factors should be considered such as availability, spatial resolution, processing time, and cost. But for many applications, data accuracy is the critical factor. This study shows that although not as precise as the USGS elevation models, ASTER DEM data is still more accurate in reflecting the current topography it covers. Some studies on ASTER DEM generation methods suggest that its accuracy could be improved and its flaws reduced (van Ede, 2004, Subramanian et al., 2003, & Cleff, 1999), but technological advancement is already ahead in producing higher accuracy elevation data at low cost, such as the SRTM (Shuttle Radar Topography Mission) data with 1-arc-second resolution and 10 meters RMSE accuracy.

## REFERENCES

- Abrams, M., S. Hook, & B. Ramachandran (2002). *ASTER User Handbook Ver. 2*. Jet Propulsion Laboratory, EROS Data Center. Retrieved November 11, 2004 from [http://asterweb.jpl.nasa.gov/documents/aster\\_user\\_guide\\_v2.pdf](http://asterweb.jpl.nasa.gov/documents/aster_user_guide_v2.pdf)
- Aniello, P. (2003). *Using ASTER DEMs to Produce IKONOS Orthophotos*. Space Imaging. EOM [Littleton] Vol. 12. No. 5. p. 22-26. Retrieved November 15, 2003 from [http://www.spaceimaging.com/whitepapers\\_pdfs/2003/pa\\_eom\\_paper\\_for\\_pdf.pdf](http://www.spaceimaging.com/whitepapers_pdfs/2003/pa_eom_paper_for_pdf.pdf)
- Breuer, M. (2002). *DEM and Orthoimage from ASTER Data*. Geosystems, Germany. Retrieved October 12, 2004 from [http://www.engesat.com.br/produtos/ASTER\\_DEMs.pdf](http://www.engesat.com.br/produtos/ASTER_DEMs.pdf)
- Chrysoulakis, N., M. Diamandakis, & P. Prastacos (2003). *GIS Integration of ASTER Stereo Imagery for the Support of Watershed Management*. 8th International Conference on Environmental Science and Technology. Lemnos island, Greece.
- Couperus, J. & B. Schmidt (2004, March). *A scar above Santa Clara County: Quarry operations threatening foothills*. Green Footnotes News. Retrieved December 15, 2004 from [http://www.greenfoothills.org/news/2004/03-2004\\_Quarry.html](http://www.greenfoothills.org/news/2004/03-2004_Quarry.html)
- Endreny, T. A., E. F. Wood, & A. Hsu (2000). *Correction of Errors in SPOT-derived DEMs using GTOPO30 Data*. In IEEE Transactions on Geoscience and Remote Sensing, Volume 38, Number 3, p 1234-1241.
- ERDAS Field Guide (1999). ERDAS Inc., Atlanta, U.S.A.
- ERSDAC (2002). *ASTER User's Guide, Part III, DEM Product*. Earth Remote Sensing Data Analysis Center, Tokyo, Japan. Retrieved November 15, 2003 from <http://www.science.aster.ersdac.or.jp>
- Gesch, D., J. Williams, & W. Miller (2001). *A Comparison of U.S. Geological Survey Seamless Elevation Models with Shuttle Radar Topography Mission Data*. International Geoscience and Remote Sensing Symposium, in IGARSS 2001; Scanning the present and resolving the future; proceedings. (Tony Milne, chairperson and others). 2001, v. 2, p. 754-756
- Honda, K. (2004). *Digital Elevation Model (DEM) Processing*. Retrieved November 12, 2004 from [http://www.star.ait.ac.th/~honda/textbooks/advrs/2.DEM\\_6pbw.pdf](http://www.star.ait.ac.th/~honda/textbooks/advrs/2.DEM_6pbw.pdf)

- Hurtado, J.M. (2002). *Extraction of a digital elevation model from ASTER Level 1A stereo imagery using PCI Geomatica OrthoEngine® v.8.2.0*. Retrieved November 12, 2004 from [http://www.gps.caltech.edu/users/fisheggs/resource/ASTER\\_DEM\\_Procedure.pdf](http://www.gps.caltech.edu/users/fisheggs/resource/ASTER_DEM_Procedure.pdf)
- Kääb, A. (2002). *Monitoring high-mountain terrain deformation from repeated air- and spaceborne optical data: examples using digital aerial imagery and ASTER data*. ISPRS Journal of Photogrammetry & Remote Sensing. 57 (1-2). 39-52.
- Kääb, A., C. Huggel, F. Paul, R. Wessels, B. Raup, H. Kieffer & J. Kargel (2003). *Glacier Monitoring from ASTER Imagery: Accuracy and Applications*. Proceedings of EARSeL-LISSIG-Workshop Observing our Cryosphere from Space, Bern, March 11 - 13, 2002. EARSeL e-Proceedings. 2. 43-53
- Lang, H. & R. Welch (1999). *Algorithm Theoretical Basis Document for ASTER Level-1 Data Processing*, ver. 3.0. Earth Remote Sensing Data Analysis Center, USA. Retrieved April 11, 2004 from [http://krsc.kari.re.kr/sub/satellite/download/satellite\\_04/ASTER/atbd-ast-08.pdf](http://krsc.kari.re.kr/sub/satellite/download/satellite_04/ASTER/atbd-ast-08.pdf)
- Leff, C. (1999). *ASTER - Higher-Level Data Product Quality Assessment Plan*, ver.2. Jet Propulsion Laboratory, California Institute of Technology, Pasadena. Retrieved June 12, 2004 from [http://asterweb.jpl.nasa.gov/documents/ASTER\\_QA\\_Plan\\_v2.0.pdf](http://asterweb.jpl.nasa.gov/documents/ASTER_QA_Plan_v2.0.pdf)
- Selby, R. (2002). *Creating Digital Elevation Models and Orthoimages from ASTER Imagery*. PCI Geomatics, United Kingdom. Retrieved April 11, 2004 from [http://www.pcigeomatics.com/support\\_center/tech\\_papers/grsg\\_aster\\_article.pdf](http://www.pcigeomatics.com/support_center/tech_papers/grsg_aster_article.pdf)
- Subramanian S., A.Singh, & M. Sudhakar (2003). *Evaluation of Digital Elevation Models created from different satellite images*. RMSI Private Limited. Retrieved June 15, 2004 from [www.gisdevelopment.net/technology/rs/pdf/79.pdf](http://www.gisdevelopment.net/technology/rs/pdf/79.pdf)
- Toutin, T., & P. Cheng (2001). *DEM generation with ASTER stereo data*. Earth Observation Magazine 10 (6), 10–13. Retrieved November 10, 2003 from <http://www.eonline.com/Common/currentissues/June01/thierry.htm>
- Toutin, T. (2002). *3D Topographic Mapping with ASTER Stereo Data in Rugged Topography*. Natural Resources Canada, Canada Centre for Remote Sensing. Retrieved November 10, 2003 from <http://www.gisdevelopment.net/technology/rs/mi03079d.htm>

- Toutin, T., & P. Cheng (2002). *Comparison of automated digital elevation model extraction results using along-track ASTER and across-track SPOT stereo images*. Optical Engineering, 41(9): 2102-2106.
- Trimble Navigation Limited (1999). GeoExplorer 3 operation guide, U.S.A.
- USGS (1998). *Retrieving and Unpacking SDTS Data*. Tutorial and Users Manual. Retrieved June 23, 2004 from <http://thor-f5.er.usgs.gov/sdts/articles/pdf/sdts-tutorial.pdf>
- USGS (1998). *Standards for Digital Elevation Models* Parts I, II, & III. National Mapping Program Technical Instructions. Retrieved November 6, 2004 from <http://fisher.lib.virginia.edu/collections/gis/dem/metadata/dem.details.html>
- USGS (2000). US GeoData Digital Elevation Models Fact Sheet 040-00. Retrieved July 15, 2004 from <http://erg.usgs.gov/isb/pubs/factsheets/fs04000.html>
- USGS (2002). *The National Map - Elevation*. Retrieved October 11, 2004 from <http://erg.usgs.gov/isb/pubs/factsheets/fs10602.pdf>
- USGS (2003). National Elevation Dataset. Retrieved October 11, 2004 from <http://ned.usgs.gov/>
- U.S. Geological Survey (USGS). Digital Elevation Model. Retrieved November 6, 2004 from <http://edc.usgs.gov/guides/dem.html>
- Van Ede, R. (2004). *Destriping and Geometric Correction of an ASTER Level 1A Image*. Retrieved November 17, 2004 from [http://home.hccnet.nl/r.v.ede/remote/ASTER report V3.PDF](http://home.hccnet.nl/r.v.ede/remote/ASTER%20report%20V3.PDF)
- Vogt, S. & J. Arigony (2002). *Ground Control Points for Satellite Imagery on King George Island*. King George Island GIS Project, SCAR GIG / IPG Univ. Freiburg.
- Wechsler, S. P. (2000). *A Methodology for Digital Elevation Model (DEM) Uncertainty Evaluation: The Effect DEM Uncertainty on Topographic Parameters*. State University of New York. Dissertation. Retrieved October 15, 2004 from <http://www.csulb.edu/~wechsler/Dissertation/DissPage.html>

## APPENDIX A

### TRIMBLE GEOEXPLORER III CONFIGURATION FOR FIELD SURVEY

**Datum:** WGS84

**PDOP Mask:** 4.0

PDOP (positional dilution of precision) is a unitless measure that quantifies the geometrical configuration of the available GPS satellites at any given time. A low PDOP is desirable. PDOP values of under 6 is the standard for US Forest Service GPS mapping activity, and 6 is also the maximum PDOP recommended by NASA for gathering GCPs.

**SNR Mask:** 7.0

SNR is the signal-to-noise ratio of each satellite. The signal strength of a satellite is a measure of the information content of the signal, relative to the signal's noise. The typical SNR of a satellite at 30° elevation is between 10.0 and 15.0. The quality of a GPS position is degraded if the SNR of one or more satellites in the constellation falls below 6.0.

**Elevation Mask:** 15 degrees

The GeoExplorer 3 can only use satellites above the specified elevation in the sky to compute GPS positions. Using an elevation mask lower than 15° could increase ionospheric noise associated with satellites low on the horizon and would counter any improvement in PDOP given by the increase of satellites captured.

**Logging interval:** 5 seconds

**Minimum satellites to compute position:** 5

**GPS height/offset:** 1 meter

Height of the GPS antenna above the feature you are collecting

## APPENDIX B

### GROUND CONTROL POINTS USED FOR ASTER ABSOLUTE DEM GENERATION

ID #	Xn	Yn	Xb	Yb	Longitude	Latitude	Elevation (meters)
1	379	3911	1154	4785	-122.127355	37.30572	784.459
2	1697	3460	2481	4256	-121.8833738	37.33469754	24.273
3	2366	1296	3149	2027	-121.68706	37.60462	418.798
4	1165	3487	1945	4327	-121.9767564	37.34365425	28.758
5	1483	4018	2267	4829	-121.94103	37.26615	71.384
6	1369	1610	3147	2433	-121.8717042	37.5865417	79
7	1871	525	2649	1306	-121.7442849	37.71807739	152.418
8	3328	1816	4114	2459	-121.5403136	37.51256577	697.65
9	1187	1076	1963	1914	-121.8833437	37.66143491	105.519
10	436	145	1203	1046	-121.9804663	37.80170024	129.318
11	226	2893	997	3813	-122.1189315	37.44391735	0.349
12	921	2987	1699	3848	-122.0006598	37.41530905	-1.093
13	1705	2602	2487	3393	-121.8499281	37.44780724	171.005
14	909	1940	1684	2803	-121.9641522	37.5537248	18.992
15	166	1639	934	2565	-122.0833945	37.6108346	3.299
16	1751	3257	2535	4049	-121.86665	37.3603319	23.746
17	1753	3561	2538	4353	-121.8775665	37.32027045	30.415
18	1897	4126	2684	4904	-121.87348	37.24225	60.11
19	329	3499	1102	4406	-122.1226508	37.3614	90.49
20	3644	3230	4435	3848	-121.54015	37.31952	703.78
21	3535	395	4320	1050	-121.45278	37.69625	52.43
22	3795	128	4580	765	-121.39822	37.72523	21.49
23	2519	3163	3307	3872	-121.7302	37.3548	563.9
24	2989	3810	3780	4491	-121.67415	37.25855	361.8

Xn, Yn: GCP location (Line and Sample values) in ASTER band 3N (nadir)

Xb, Yb: GCP location (Line and Sample values) in ASTER band 3B (backward)